

# Linear diode laser bar optical stretchers for cell deformation

Ihab Sraj,<sup>1</sup> David W.M. Marr,<sup>2</sup> and Charles D. Eggleton<sup>1,\*</sup>

<sup>1</sup>*Department of Mechanical Engineering, University of Maryland Baltimore County,  
Baltimore, Maryland 21250, USA*

<sup>2</sup>*Department of Chemical Engineering, Colorado School of Mines,  
Golden, Colorado 80401, USA*

*\*eggleton@umbc.edu*

**Abstract:** To investigate the use of linear diode laser bars to optically stretch cells and measure their mechanical properties, we present numerical simulations using the immersed boundary method (IBM) coupled with classic ray optics. Cells are considered as three-dimensional (3D) spherical elastic capsules immersed in a fluid subjected to both optical and hydrodynamic forces in a periodic domain. We simulate cell deformation induced by both single and dual diode laser bar configurations and show that a single diode laser bar induces significant stretching but also induces cell translation of speed  $< 10 \mu\text{m/sec}$  for applied  $6.6 \text{ mW}/\mu\text{m}$  power in unconfined systems. The dual diode laser bar configuration, however, can be used to both stretch and optically trap cells at a fixed position. The net cell deformation was found to be a function of the total laser power and not the power distribution between single or dual diode laser bar configurations.

©2010 Optical Society of America

**OCIS codes:** (170.1530) Cell analysis; (140.2020) Diode lasers; (140.7010) Laser trapping; (000.4430) Numerical approximation and analysis.

---

## References and links

1. A. Ashkin, "Acceleration and trapping of particles by radiation pressure," *Phys. Rev. Lett.* **24**(4), 156–159 (1970).
2. A. Ashkin, J. M. Dziedzic, and T. Yamane, "Optical trapping and manipulation of single cells using infrared laser beams," *Nature* **330**(6150), 769–771 (1987).
3. J. Guck, S. Schinkinger, B. Lincoln, F. Wottawah, S. Ebert, M. Romeyke, D. Lenz, H. M. Erickson, R. Ananthakrishnan, D. Mitchell, J. Käs, S. Ulvick, and C. Bilby, "Optical deformability as an inherent cell marker for testing malignant transformation and metastatic competence," *Biophys. J.* **88**(5), 3689–3698 (2005).
4. G. Bao, and S. Suresh, "Cell and molecular mechanics of biological materials," *Nat. Mater.* **2**(11), 715–725 (2003).
5. J. Guck, R. Ananthakrishnan, H. Mahmood, T. J. Moon, C. C. Cunningham, and J. Käs, "The optical stretcher: a novel laser tool to micromanipulate cells," *Biophys. J.* **81**(2), 767–784 (2001).
6. M. Gu, S. Kuriakose, and X. Gan, "A single beam near-field laser trap for optical stretching, folding and rotation of erythrocytes," *Opt. Express* **15**(3), 1369–1375 (2007).
7. S. K. Mohanty, A. Uppal, and P. K. Gupta, "Self-rotation of red blood cells in optical tweezers: prospects for high throughput malaria diagnosis," *Biotechnol. Lett.* **26**(12), 971–974 (2004).
8. R. R. Huruta, M. L. Barjas-Castro, S. T. O. Saad, F. F. Costa, A. Fontes, L. C. Barbosa, and C. L. Cesar, "Mechanical properties of stored red blood cells using optical tweezers," *Blood* **92**(8), 2975–2977 (1998).
9. S. Hénon, G. Lenormand, A. Richert, and F. Gallet, "A new determination of the shear modulus of the human erythrocyte membrane using optical tweezers," *Biophys. J.* **76**(2), 1145–1151 (1999).
10. P. J. H. Bronkhorst, G. J. Streekstra, J. Grimbergen, E. J. Nijhof, J. J. Sixma, and G. J. Brakenhoff, "A new method to study shape recovery of red blood cells using multiple optical trapping," *Biophys. J.* **69**(5), 1666–1673 (1995).
11. P. B. Bareil, Y. Sheng, Y. Q. Chen, and A. Chiou, "Calculation of spherical red blood cell deformation in a dual-beam optical stretcher," *Opt. Express* **15**(24), 16029–16034 (2007).
12. G. B. Liao, P. B. Bareil, Y. Sheng, and A. Chiou, "One-dimensional jumping optical tweezers for optical stretching of bi-concave human red blood cells," *Opt. Express* **16**(3), 1996–2004 (2008).
13. R. W. Applegate, J. Squier, T. Vestad, J. Oakey, and D. W. M. Marr, "Fiber-focused diode bar optical trapping for microfluidic flow manipulation," *Appl. Phys. Lett.* **92**(1), 013904 (2008).
14. I. Sraj, J. Chichester, E. Hoover, R. Jimenez, J. Squier, C. D. Eggleton, and D. W. M. Marr, "Cell deformation cytometry using diode-bar optical stretchers," *J. Biomed. Opt.* **15**, (2010), in press.

15. C. Peskin, and D. McQueen, "A three dimensional computational method for blood flow in the heart I. immersed elastic fibers in a viscous incompressible fluid," *J. Comput. Phys.* **81**(2), 372–405 (1989).
  16. C. D. Eggleton, and A. S. Popel, "A large deformation of red blood cell ghosts in a simple shear flow," *Phys. Fluids* **10**(8), 1834–1845 (1998).
  17. P. Pawar, S. Jadhav, C. D. Eggleton, and K. Konstantopoulos, "Roles of cell and microvillus deformation and receptor-ligand binding kinetics in cell rolling," *Am. J. Physiol. Heart Circ. Physiol.* **295**(4), 1439–1450 (2008).
  18. C. Peskin, "Numerical analysis of blood flow in the heart," *J. Comput. Phys.* **25**(3), 220–252 (1977).
  19. A. Ashkin, "Forces of a single-beam gradient laser trap on a dielectric sphere in the ray optics regime," *Biophys. J.* **61**(2), 569–582 (1992).
  20. J. Guck, R. Ananthakrishnan, T. J. Moon, C. C. Cunningham, and J. Käs, "Optical deformability of soft biological dielectrics," *Phys. Rev. Lett.* **84**(23), 5451–5454 (2000).
  21. P. B. Bareil, Y. Sheng, and A. Chiou, "Local stress distribution on the surface of a spherical cell in an optical stretcher," *Opt. Express* **14**(25), 12503–12509 (2006).
  22. H. C. Van de Hulst, "Light scattering by small particles," John Wiley and Sons, New York. 172–176 (1957).
- 

## 1. Introduction

In 1970, Ashkin demonstrated optical trapping as a non-contact manipulation technique [1]. In this, a single laser beam is focused to a diffraction-limited spot with high numerical-aperture optics allowing micron-sized particles or cells [2] to be trapped in solution. Recently, the technique has been extended beyond the simple trapping of cells to the direct probe of individual cell properties [3] and their deformation [4], stretching [5], folding, and rotation [6,7]. To extract quantitative information from this, different approaches have been employed including drag-based deformation [8], attaching beads [9], or multiple optical tweezers to deform individual cells [10–12]. Käs and associates have recently developed an optical trapping based stretcher in which they trap individual cells along a single axis between two counter-propagating diverging beams [5,11]. All of these techniques have demonstrated the utility and advantage of optical trapping for determining cell deformability; however, they do not lend themselves to high-throughput measurement as they focus on individual cells within static systems. More recently, Applegate *et al.* have implemented a significantly simplified optical trapping method that employs linear diode laser bars to induce optical forces within confining microfluidic systems of speed 300–700  $\mu\text{m/s}$  depending on particle size [13]. This approach uses only a single bar-shaped laser beam for cell manipulation and sorting within flowing systems, eliminating the need for expensive associated optics to provide an easily integrated tool within microscale platforms. In recent work, Sraj *et al.* used this technique to both deform and stretch cells at a speed of 50  $\mu\text{m/s}$  [14].

In this manuscript, we simulate the implementation of these linear optical sources for inducing deformation as optical stretchers. Here we compare their use in a single linear diode laser bar configuration and an opposed dual-bar configuration to determine the relative effectiveness of applying individual versus opposing force configurations. The numerical method we employ is the immersed boundary method (IBM) introduced by Peskin [15], used extensively to simulate fluid-structure interaction in biological systems [15–18], but now coupled with a ray-optics technique [5,19]. In the IBM, a finite element model of the capsule membrane is used to relate local membrane forces to local membrane deformation. Details of the numerical implementation and validation of our model can be found in our previous work [16]. Here, the initial force distribution is found using the governed mathematical model [5], now applied to the cell membrane where deformation is observed.

## 2. Numerical method

We model the cell membrane as an infinitely thin hyperelastic neo-Hookean material with negligible bending resistance. The neo-Hookean elastic model is commonly used for capsule deformation due to its simplicity and is characterized solely by the membrane stiffness  $Eh$  [16]. An unstressed spherical cell of initial radius  $a$  is first placed in an incompressible Newtonian fluid with the same density  $\rho$  and viscosity  $\mu$  as the cytoplasmic fluid but with a different index of refraction. The diode laser bar emits light that induces optical forces on the cell surface due to the refractive index mismatch and the resulting light refraction and reflection at the interface. This leads to a transient cell deformation until membrane elastic

forces balance the applied optical forces unless the applied load is too large, in which case the cell membrane will rupture. In addition, this induced transient deformation of the cell induces fluid flow that, in turn, leads to viscous stresses that influence the characteristic time for capsule deformation:

$$t_0 = \frac{\mu a^2}{F_{optical}}. \quad (1)$$

Modeling of cell optical stretching forces has only recently been discussed [20,21]. In our work, the traditional ray optics approach used to determine the optical forces on large spherical systems is extended to calculation of local stress profiles across the front and back sphere surfaces as a function of refractive index and incident laser beam profile. This approach is valid when the object is much larger than the wavelength of the light [22]. For spherical objects this condition is given by  $2\pi a/\lambda \gg 1$  where  $\lambda$  is the laser wavelength. For cells of radius greater than 3  $\mu\text{m}$  and laser wavelengths less than 1  $\mu\text{m}$  this condition is satisfied [5]. Commercially available linear diode laser bars 1  $\mu\text{m}$  in width consist of a number of individual emitters along the length of the diode bar separated by a finite gap. These individual sources emit light with a small divergence angle, generally  $\sim 10^\circ$ . To simplify our ray optics calculations, we model the diode laser bar light source as an infinite number of parallel rays, an approximation that works well for these small divergence angles. As the rays refract, change in path leads to a change in the momentum carried by the light that is transferred to the interface through conservation. When the interface is an object, its surface absorbs this momentum and experiences a force proportional to the laser power via Newton's 2nd law. Multiple reflections are neglected here as their effects rapidly diminish with the reflectance  $R < 0.005$  for all rays. To simplify calculation we consider the front and back surface of the cell separately. The parallel ray hits the front surface of sphere with an angle  $\alpha$  and the refracted angle found using Snell's law,  $n_1 \sin \alpha = n_2 \sin \beta$ , as illustrated in Fig. 1(a) and detailed in [21]. The calculated optical forces imposed by the diode laser bar optical stretchers are integrated into the IBM by applying them on the nodes of the fully 3D membrane finite element grid. These forces are assumed constant as the cell deforms [5].

The net optical force  $F_{optical}$  on a cell surface can be written in this form:

$$F_{optical} = \frac{n_m P Q}{c}, \quad (2)$$

where  $n_m$  is the buffer medium index of refraction,  $P$  the total laser power,  $Q$  the dimensionless trapping efficiency and  $c$  the speed of light in vacuum. For simplicity  $Q$  is calculated following [5] where it is decomposed into two components (parallel and perpendicular to the laser axis) as follows:

$$\begin{aligned} Q_{front}^{\parallel}(\alpha) &= 1 + R(\alpha) \cos(2\alpha) - n(1 - R(\alpha)) \cos(\alpha - \beta) \\ Q_{front}^{\perp}(\alpha) &= R(\alpha) \sin(2\alpha) - n(1 - R(\alpha)) \sin(\alpha - \beta) \end{aligned} \quad (3)$$

$$\begin{aligned} Q_{back}^{\parallel}(\alpha) &= (1 - R(\alpha)) [n \cos(\alpha - \beta) + nR(\beta) \cos(3\beta - \alpha) - (1 - R(\beta)) \cos(2\alpha - 2\beta)] \\ Q_{back}^{\perp}(\alpha) &= (1 - R(\alpha)) [-n \sin(\alpha - \beta) + nR(\beta) \sin(3\beta - \alpha) - (1 - R(\beta)) \sin(2\alpha - 2\beta)], \end{aligned} \quad (4)$$

where  $n = n_p / n_m$  and  $n_p$  is the cell's refractive index. The magnitude of trapping efficiency

$Q$  at any point is then found using  $Q = \sqrt{(Q^{\perp})^2 + (Q^{\parallel})^2}$  and the total trapping efficiency and corresponding total force can be found through surface integration.

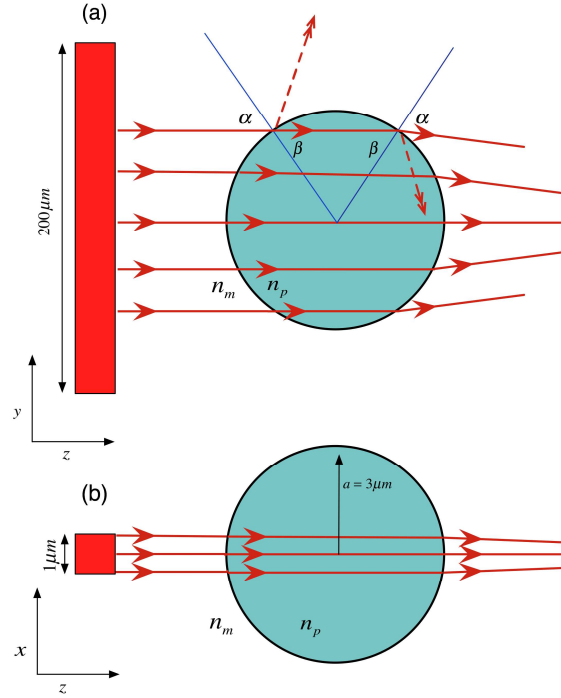


Fig. 1. Model of the diode laser bar geometry used and the ray optics approach on a spherical cell in the (a) y-z plane and (b) x-z plane. The position and dimension of the diodes are not drawn to scale

Cell deformation (asymmetry) is characterized by the Taylor deformation parameter,

$$DF = \frac{A - B}{A + B} \quad (5)$$

where  $A$  and  $B$  are the lengths of the major and minor axes of elongated cells. The deformation parameter  $DF$  does not describe the local strain distribution within the capsule membrane but instead provides a macroscopic description of the state of capsule deformation.

### 3. Physical and computational values

We consider a 3D elastic spherical capsule of radius  $a = 3 \mu\text{m}$  using a neo-Hookean elastic model of membrane stiffness  $Eh = 0.1 \text{ dyne/cm}$ . The cell is immersed in a homogeneous fluid having the properties of water with a density  $\rho = 1 \text{ g/cm}^3$  and dynamic viscosity  $\mu = 0.8 \text{ cP}$ . The index of refraction is 1.37 for the fluid inside the cell and 1.33 outside the cell. The optical source is a linear diode laser bar of dimension  $200 \times 1 \mu\text{m}^2$  [Fig. 1(a) and (b)] and  $\lambda = 833 \text{ nm}$  [13,14]. The  $200 \mu\text{m}$  length lies in the y-axis and the laser beam direction is along the z-axis. The induced optical forces from Eqs. (3) and (4) are in the x-z plane. Figure 2(a) and 2(b) provide a 2D side view and color map of the optical stress distribution on a 3D cell membrane in single and symmetric dual diode laser bar configurations at the same total laser power. The centerline of the  $1 \mu\text{m}$  wide optical beam from the diode laser bar (red square) intersects the cell equator [see Fig. 1(b)]. The long axis of length  $200 \mu\text{m}$  is in and out of the plane. As expected, a single diode laser bar produces a net translating force,  $F_{\text{optical}}$  in the z-direction, pushing the cell away from the light source [Fig. 2(a)]. For the dual trap case, the diode laser bars are positioned symmetrically on opposite sides of the cell in the same plane and the total net force is zero; however the cell is now subjected to stretching forces on both the front and back sides [Fig. 2(b)]. The fluid domain is a cube with a side that is  $8 \times$  the cell radius with periodic boundary conditions. The uniform grid used in the simulations has  $64^3$

nodes with a grid spacing of  $a/8$  while the finite element cell grid has 25600 triangular elements. A time step of  $10^{-5}$  sec was used to ensure numerical stability.

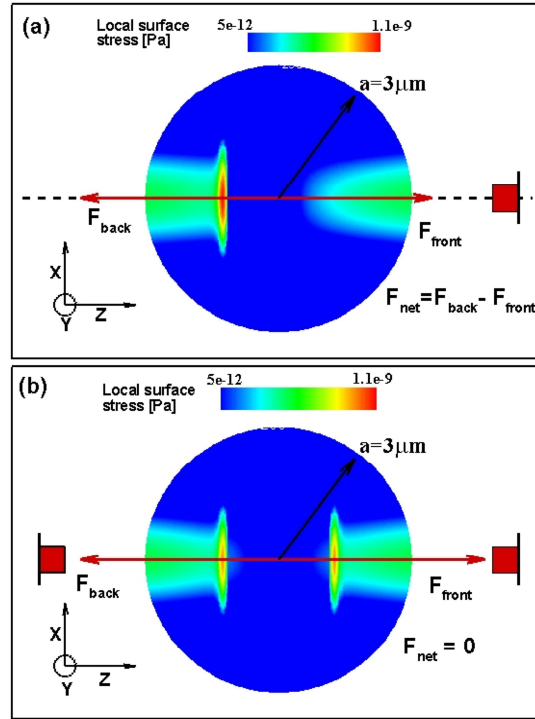


Fig. 2. 2D side view of the optical stress distribution color map on a 3D cell membrane of radius  $a$  from a  $1 \mu\text{m}$  wide (a) single diode laser bar (red square) with long axis in and out of the figure along the  $y$ -direction. The net force is pushing the cell away from the diode laser bar and (b) symmetric dual diode laser bars (both with long axes along the  $y$ -direction) where the cell does not translate. The total optical power is the same for both cases but the maximum local surface stress for case (a) is twice that of case (b). The arrows indicate the direction of back and front translational force. The position and dimension of the diodes are not drawn to scale.

#### 4. Results and discussion

Cell deformation, quantified by the Taylor parameter  $DF$ , is simulated for  $0 < t^* = t/t_0 \leq 1$  insuring a steady-state shape is reached for the different diode configurations. The total diode optical power is varied for both single and dual diode laser bar configurations. Figure 3(a) shows the evolution of  $DF$  as a function of the dimensionless time,  $t^*$ , using single and symmetric dual diode laser bar optical stretchers for different laser powers. The characteristic time,  $t_0$ , for a  $6.6 \text{ mW}/\mu\text{m}$  laser power is 12 ms and, using a time step of 0.01 ms,  $\sim 1200$  time steps were required to reach a steady-state shape. In the case of a  $106 \text{ mW}/\mu\text{m}$  laser,  $t_0 = 0.75$  ms and only 75 time steps were required. As expected, the equilibrium deformation increases with the applied laser power. In these calculations, we note that a single diode laser bar both deforms the model cell and imparts a net translation force and cell movement. Here, the single diode laser bar and the symmetric dual diode laser bar deformation profiles are similar for the same total laser power. In Fig. 3(b) we plot the equilibrium deformation  $DF_\infty$  as a function of the net applied optical force,  $F_{\text{optical}}$  where, in the case of fixed cell parameters,  $F_{\text{optical}}$  is an indication of the total optical power used. We clearly see from Fig. 3(b) that the total optical power is the dominant parameter and not the diode laser bar number.

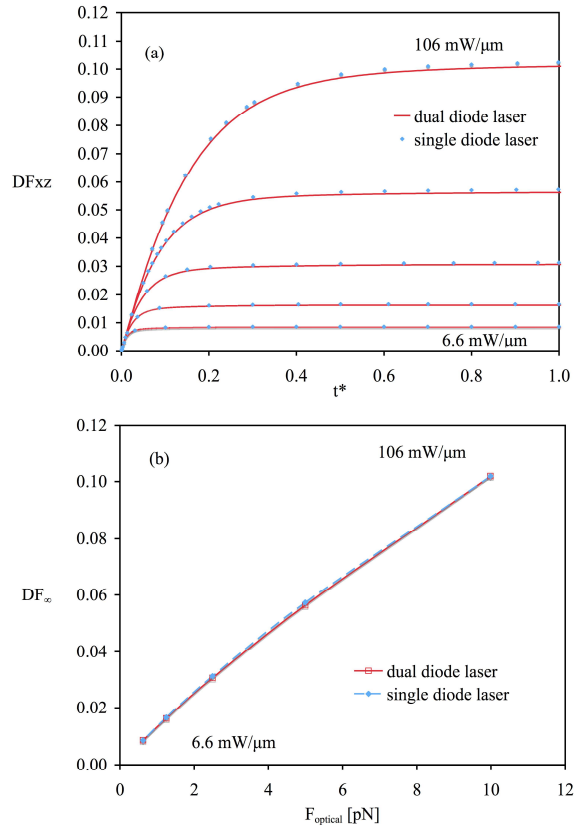


Fig. 3. (a) Evolution of deformation parameter  $DF$  as a function of time for different diode laser power using single and dual diode laser bars. Total laser power is held fixed by setting the power in each diode laser in the dual configuration to half the power of the single diode laser case. For the physical properties provided in the text, the asymptotic values  $DF_{\infty}$  range from 0.008 using a 6.6 mW/ $\mu\text{m}$  diode laser ( $F_{\text{optical}} = 0.62$  pN) to 0.11 using a 106 mW/ $\mu\text{m}$  diode laser ( $F_{\text{optical}} = 9.98$  pN). (b) Variation of equilibrium deformation parameter  $DF_{\infty}$  as a function of the net optical force  $F_{\text{optical}}$  for different optical stretcher cases. Lines are guides to the eye.

To investigate cell movement for the case of a single diode laser bar, we calculate the cell translational speed at steady state (terminal speed). For the lowest laser power used, 6.6 mW/ $\mu\text{m}$ , the computed net optical force  $F_{\text{optical}}$  is 0.62 pN which could lead to cell translations in the direction of laser beam (z-axis) of  $\sim 9$   $\mu\text{m}/\text{sec}$  at steady state in unconfined systems, assuming simple Stokes drag. Higher laser powers of 106 mW/ $\mu\text{m}$  provide  $F_{\text{optical}}$  of 9.98 pN and theoretical cell speeds of  $\sim 160$   $\mu\text{m}/\text{sec}$ .

Figure 4(a) and Fig. 4(b) illustrate the steady-state deformed shapes induced by both single and symmetric dual diode laser bar optical stretchers. Note that in the single diode case, translation of the cell is apparent over the time scale of the applied stretching forces. From these and the quantitative values of Fig. 3, the steady-state deformation of the cell depends on the total power but appears independent of the power distribution. This result is certainly valid for smaller applied stretching forces and at small deformations but will break down as the front of the cell is significantly deformed and our assumption of constant applied stretching forces becomes invalid. In this, the changing refraction at the cell front will broaden the stretching profile on the backside of the cell, leading to significant asymmetry in the force distribution. Though simulations that take this into account are certainly feasible, most experimental efforts aimed at determining cell stiffness will occur at lower applied optical powers with smaller induced deformations where any possible impact of the stretching on cell properties is minimized.

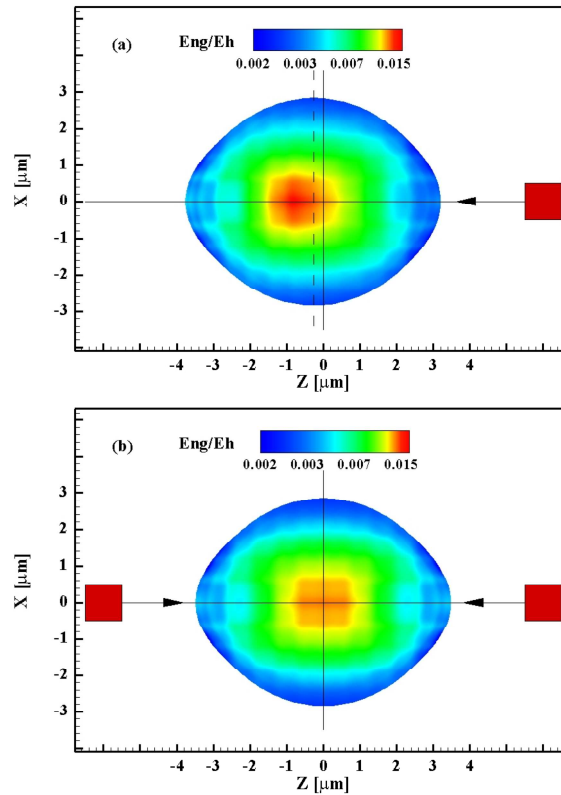


Fig. 4. Side view of the deformed cell at steady-state from a fully 3-D simulation colored by the elastic energy distribution,  $Eng$ , normalized by  $Eh$  using (a) single diode of 53.3 mW/ $\mu m$  power and (b) symmetric dual diodes of 26.6 mW/ $\mu m$  power each. Total energy is the same but is more localized in the case of the single diode.

## 5. Conclusions

In this paper, we simulate the transient cell deformation induced by single and dual linear diode laser bar optical stretchers. We compare the deformation and relaxation by applying increasing optical forces and power distributions on a spherical cell with neo-Hookean membrane properties. Our simulations show that the forces imposed by a single diode laser bar optical stretcher can be used to both deform and translate cells immersed in fluid. Because single source configurations require no alignment, implementation of single diode optical stretchers where small translational forces can be tolerated will greatly simplify measurement of cell deformation in high-throughput applications.

## Acknowledgments

The authors would like to acknowledge financial support provided by the National Institute of Health grants R01 AI063366 and R01 AI079347-01.